" MHD COUETTE FLOW OF MICROPOLAR CASSON FLUID WITH HEAT TRANSFER USING CUBIC-B SPLINE APPROXIMATION: A NUMERICAL APPROACH"

Vinay Sharma[1*], Rajesh Kumar Chandrawat[2], Deepak Kumar[3]

Abstract –
Micropolar Casson fluids exhibit complex rheological properties due to the presence of microstructure and has the potential of getting used in many fields, including biomedical engineering, materials science, industrial processes, aerospace engineering, and environmental engineering. The current study examines, the behavior of micropolar Casson fluids in a horizontal channel with heat transmission when a magnetic field is applied. Fluid flow in a channel is driven and maintained by the motion of the upper plate with constant linear velocity. The flow behavior is studied under different conditions, including changes in the Casson micropolar parameter, micropolar parameter and Hall parameter. The differential quadrature approach is employed with modified cubic-B spline (MCB-DQM) to solve the reduced non-dimensional governing partial differential equations for calculating the microrotation, temperatures and velocities profiles under acceptable physically boundary and interfacial conditions. The study identified the impact of various fluid parameters on linear velocity, microrotation and temperature profiles. It has been noted that an increment in the Casson micropolar, micropolar, and Hall parameters results in an increment in microrotation and velocity profiles, while an increase in the Reynolds number and square of Hartmann number results in a reduction in these profiles. Also, Temperature profile varies inversely with an increment in the time, square of Hartmann number, micropolar, Casson micropolar and Hall parameters, but may increase with the Prandtl number, Eckert and Reynolds number. The study's findings reveal a scientific basis for the development and optimization of numerical models and simulations for predicting fluid flow and heat transfer in different systems like design of microfluidic devices, electronic cooling systems, and material processing techniques, leading to improved performance and efficiency.

Keywords **–**Casson Micropolar Fluid, Couette Flow. Unsteady Flow, Differential Quadrature Method, Modified Cubic B-Spline, Magnetohydrodynamics.

[1*]Department of Applied Science & Humanities (Mathematics), Govt. Hydro Engineering College, Bandla, Bilaspur, Himachal Pradesh, India & Research scholar at Lovely Professional University, Phagwara, Jalandhar, Punjab, India.
[2] School of Engineering and Information Technology, Manipal Academy of Higher Education Dubai.
[3] Department of Mathematics, Lovely Professional University Jalandhar, 144411, India.

***Corresponding author:-** Vinay Sharma
*Department of Applied Science & Humanities (Mathematics), Govt. Hydro Engineering College, Bandla, Bilaspur, Himachal Pradesh, India & Research scholar at Lovely Professional University, Phagwara, Jalandhar, Punjab, India Email:- vinaysharma77@gmail.com

DOI: 10.48047/ecb/2023.12.si10.00485

NOMENCLATURE

σ	fluids Electrical conductivity in S/m
J	Current density in Am^{-2}
B_0	Magnetic field in A/m
Be	Hall parameter
Bi	Ion slip parameter
u_{cm}	Fluid velocity in m/s
$T_{lp}\ T_{up}$	Temperatures at lower and upper plates in K
M_{cm}	Fluid angular velocity in S^{-1}
T_{cm}	Fluid temperatures of fluid in K
ρ_{cm}	Fluid density in Kg/m^3
μ_{cm}	Viscosity co-efficient in $kg\ \cdot m^{-1} \cdot s^{-1}$
κ_{cm}	Micropolar vortex viscosities
K_{cm}	Thermal conductivity in $W/m\ \cdot K$
j_{cm}	Gyration parameters
C_{Pcm}	Specific heat capacities in $J\cdot\ kg^{-1} \cdot K^{-1}$
$\gamma_{cm}\ \beta_{cm}$	Fluid's Gyro-viscosity coefficients
K	Stokes drag coefficient
Re	Reynolds number
η_{cm}	Fluid micropolar material parameter
Ha^2	Hartmann magnetic number Square
Ec	Eckert number
Pr	Prandtl number
U_0	Velocity of upper plate of the channel

1 INTRODUCTION

Micropolar fluids are a type of non-Newtonian fluids that has microstructure and can exhibit both rotational and translational motion. Casson fluid is another type of non-Newtonian fluid that has a yield stress. Micropolar Casson fluid is a combination of both of these types of fluids. It is a fluid that is not Newtonian and features both the microstructural behavior of micropolar fluids and the yield stress behavior of Casson fluids. Micropolar Casson fluid is used to model a wide range of industrial applications, such as lubricants, polymers, and biological fluids. which means that it requires a certain amount of stress to be applied before it begins to flow. Z. Mehmood et al. [1] studied the effects of microrotation on the mixed convection flow of Casson micropolar fluid caused by a stretching sheet. The influence of parameter variation was analyzed for strong and weak concentrations of microelements. Results showed that weak concentration resulted in lower skin friction and heat flux near the wall compared to strong concentration. The primary objective of the study carried out by S. M. Upadhya et al. [2] was to monitor the induced entropy production trough an inclined microchannel by Casson-micropolar hybrid nanofluid. The study's noteworthy discovery was that the fluid temperature at the microchannel centre decreases as radiation increases. Additionally, it appears from an analysis of the Bejan number profiles that the centre of the microchannel is dominated by irreversible heat transfer. N. Abbas and W. Shatanawi [3] established a relationship between the velocity profile and the Casson micropolar parameter by examining the impact of the latter on the former in reference to study over nonlinear vertical stretching Riga sheet for flow of micropolar Casson nanofluid. The findings of the study indicated a direct correlation between the two variables. M. D. Shamshuddin and W. Ibrahim [4] in their study on "impact of a rotating system on the steady electro-magnetohydrodynamic flow of a micropolar nanofluid, which is passing through parallel plates and also affected by reactive Casson fluid". Study revealed that the transfer of momentum and angular momentum becomes more gradual or continuous as the Casson parameter increases. The investigation conducted by N. A. M. Noor et al.[5] analyzed the chemical reaction's effects on the magnetohydrodynamic Casson fluid squeeze flow over a permeable medium, while considering factors such as slip condition and viscous dissipation. The observation was made that thermal transfer rate and temperature are elevated by viscous dissipation, and in destructive chemical reactions, mass transfer rate is increased while in constructive chemical reactions it is decreased. The flow behavior of Casson fluid under MHD and mixed convection was studied by Z. Iqbal and M. Saleem [6].

The research examined the heat transfer within the flow, considering the influence of viscous dissipation and Joule heating. It was observed that an increment in the Eckert number resulted in a significant elevation of

thermal transport in the flow, while higher Hartmann numbers caused a reduction in flow velocity. to B. V. Shilpa et al. [7] utilized an analytical approach investigate the impact of Dufour and Soret numbers on the Casson fluid mixed convection flow in the presence of a porous media, uniform magnetic field and stretching in porous channel. The numerical results showed that the effects of Dufour number, Soret number, and Reynolds number was positive on the velocity, temperature, and concentration profiles.

Couette flow is a flow configuration characterized by laminar or turbulent flow within two plates parallel to each other, with one of them stationary and the second moving with uniform velocity. This results in a shear stress being generated within the fluid, causing it to flow in a parallel manner. Couette flow is commonly used as a model system to study fluid dynamics and rheology. F. Hussain et al. [8] studied the Casson nanofluid's Couette flow in a vertical channel, containing a porous medium and variable viscosity. Results on the Casson nanofluid's flow characteristics were graphically represented. It was found that the solid volume fraction parameter and porous parameter both reduce the fluid's flow and temperature.. A non-Newtonian Casson-Williamson fluid was used in a study by B. J. Gireesha and L. Anitha [9] to investigate the flow and heat transmission characteristics in an erect microchannel. The study examined the impacts of convective boundary conditions, Couette-Poiseuille flow, and nonlinear radiation in addition to evaluating entropy generation. The results demonstrated that Casson fluid exhibits a significantly higher rate of heat transfer compared to Williamson fluid. S. Gajbhiye et al. [10] investigated "the generalized Couette flow of two immiscible fluids with different viscosities between two infinite parallel plates under a constant pressure gradient and the presence of electroosmosis". The research results were displayed graphically to demonstrate the effect of various relevant flow parameters. The study concluded that the profiles for velocity and temperature shows decrement with increment in radiation parameter and Hartmann number, while an enhancement in the parameter of chemical reaction increases the concentration of two fluids. In their research, P. Mondal et al. [11] investigated "the flow, heat transfer, and entropy generation in a vertical microchannel consisting of two porous plates positioned parallel to each other". They studied the effects of both buoyancy force and transverse magnetic field, while taking into account the variable pressure gradient resulting from Couette-Poiseuille flow. Unsteady flow is the fluid motion in which the flow parameters, such as velocity, pressure, and temperature, vary with respect to time. These flows find application in field like aerodynamics, biomedical engineering and environmental engineering etc. "The effect of nonlinear radiation on the stagnation point flow of unsteady compressible Casson hybrid nanofluid over a vertically stretching sheet" was analyzed by N. Abbas et al. [12]. The study revealed that the rise in solid nanoparticle concentration resulted in a rise in the value of skin friction and a decrease in temperature gradient. This can be explained by the increased opposition to fluid motion resulted by higher concentrations of solid nanoparticles, leading to an increase in skin friction. A numerical analysis was conducted by N. Abbas et al. [13] for the flow of micropolar fluid which is magnetized, over a surface that is curved, taking into account its time-dependence. The study revealed the improved heat transfer rate for incremented value of Biot number. Theoretical investigation of "the boundary layer flow of an incompressible micropolar fluid subjected to a uniform magnetic field and driven by the buoyancy force between vertical walls" was conducted by H. R. Kataria et al.[14]. The non-dimensionalized governing equations for micropolar fluid representing unstable boundary layer momentum, rotational momentum and energy were numerically solved. Graphical illustrations were presented to demonstrate the profiles of velocity, micro-rotation, and temperature with respect to different fluid parameters. B. Widodo et al.[15] examined unstable boundary layer magnetohydrodynamic heat transport in micropolar fluid across a sphere. The results showed that an increase in the magnetic variable and micropolar parameter resulted in higher velocity profiles. However, an increase in both these values led to a decrease in the value of microrotation. R. Kodi and O. Mopuri [16] performed a study on the Casson fluid's erratic hydrodynamic movement over an elevated plate contained in a porous media, subjected to chemical reaction and Soret-aligned magnetic field. The study pointed that the velocity reduces with a rise in the angle of inclination, Casson fluid and aligned magnetic field parameter. H. R. Patel [17] conducted a study on the time dependent Casson fluid flow with free convective in a porous medium with motion characterized by quadratic speed. Analysis was done on how the properties of heat and mass transmission are affected by thermal diffusion, heat generation, chemical reaction, and thermal radiation. The study found that the coefficient of skin friction gets reduced by the presence of chemical reaction and fluid porosity, while the magnetic field and Casson parameter produced the opposite effect.

Magnetohydrodynamics (MHD) is a branch of fluid dynamics that investigates how magnetic fields affect the behaviour of electrically conductive fluids. MHD flow is used in a variety of contexts in various fields such as astrophysics, plasma physics, nuclear engineering, and geophysics etc. An investigation into "steady laminar MHD natural convection flow of suspended micropolar Casson fluid over a solid sphere" was conducted by H. T. Alkasasbeh [18]. The study revealed that a rise in the Casson parameter resulted in an increment in the

rotational velocity and local Nusselt number profiles, while the velocity, temperature and local skin friction coefficient profiles reduces. When thermal radiation and a non-uniform heat source or sink are present, the impact of an angled magnetic field on Casson nanofluid over a stretched sheet contained in a saturated porous matrix was examined by L. Panigrahi et al. [19]. The appropriate selection and accurate modelling of the fluid system is critical for the effective conclusion of the study. More recent studies on MHD flow can be seen in [20]–[23]

PDEs are crucial in fluid flow modeling, especially for complex flows where the Navier-Stokes equations cannot be solved analytically. They describe the behavior of fluids in space and time, providing a fundamental framework for understanding fluid behavior and designing new technologies. The differential quadrature approach (DQA) is a numerical method that discretizes the solution domain into a set of discrete points and at neighboring points weighted sum of function values is used to approximate derivatives. The cubic B-spline method constructs a piecewise cubic polynomial function by connecting cubic B-spline basis functions, making it a powerful tool for discretizing the solution domain in numerical methods, including the DQA method. Its flexibility and accuracy have led to its widespread application in many scientific and engineering sectors. In this work R. C. Mittal and R. Rohila [24] utilized the differential quadrature method with modified cubic B-spline function to obtain mathematical solutions for single dimensional reaction-diffusion systems. The approach involved to discretize space was the cubic B-spline, resulting in a system of ordinary differential equations. G. Arora and B. K. Singh [25] introduced the "differential quadrature method with modified cubic-B-spline (MCB-DQM)" for solving Burger's equation. The method involved the use of MCB-DQM for space discretization and an optimized Runge-Kutta with third order and four levels scheme with high stability preservation (SSP-RK43) scheme for solving the system of ordinary differential equations in time. The results showed that the proposed method outperformed other existing schemes in the literature and produced accurate results that approached the exact solutions.

The study of Casson micropolar fluid flow hold significance due to its potential applications in diverse fields. It can impact polymer processing, biomedical engineering, the oil and gas industry, magnetic material processing, and thermal management in electronics. However, the investigation of Casson micropolar fluid Couette flow in the horizontal channel under the influence of magnetic field was not adequately explored. Therefore, in this present study, we aim to address this research gap by examining the impact of fluid parameters and magnetic field on the microrotation, temperature and velocity for the aforementioned flow. Through our investigation, we seek to gain a better understanding of the fundamental behavior of this flow, as well as its practical applications in various engineering systems.

2 FORMULATION OF FLUID FLOW PROBLEM

In the case of a horizontal channel with a micropolar Casson fluid flow that is not uniform, the following assumptions are considered as shown in Figure 1:-

I. The fluid flows unidirectionally in a horizontal channel between two parallel plates, namely the lower and upper plates and is assumed to be incompressible.
II. The channel's walls are k units apart. In terms of temperature, the moving top plate is located at $y = k$ with constant temperature T_{up}, whereas the fixed bottom wall is located at $y = 0$ with constant temperature T_{lp}.
III. The upper plate maintains a steady speed of U_0, as it moves.
IV. The two walls of the channel are positioned in the X-Z.
V. The fluid experiences a uniform and static externally applied magnetic field, represented by B_0, which is aligned along the y-axis.
VI. The Lorentz force acts normal to the magnetic field applied externally and causes resistance to fluid flow in the presence of a transverse magnetic field. This body force acts on both fluids and is given by: [26]

$$J \times B_0 = \frac{\sigma {B_0}^2 (1+Bi.Be) u_{cm}}{(1+Bi.Be)^2+Be^2} \quad (1)$$

The aforementioned parameters are denoted as follows: J for current density B_0 for the externally applied magnetic field, σ for electric conductivity, Bi for the ion slip parameter and Be for the Hall parameter.

VII. In present fluid model, the micropolar Casson fluid occupies the channel for variation in y between 0 and k, with fluid velocity u_{cm}, microrotation M_{cm}, viscosity μ_{cm}, density ρ_{cm}, gyro-viscosities γ_{cm} and β_{cm}, vortex viscosity κ_{cm}, thermal conductivity K_{cm}, gyration parameter j_{cm} and specific heat capacity C_{Pcm}.
VIII. Body forces and couples are not considered.

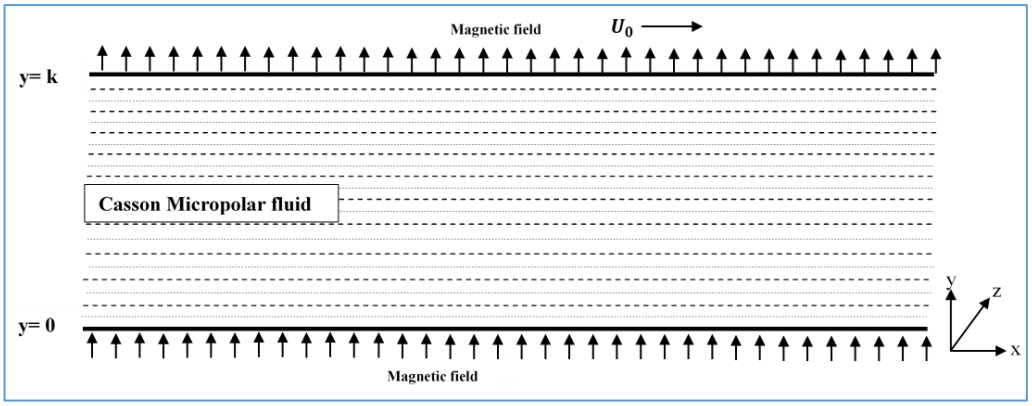

Figure 1: *Geometry of MHD Couette flow of Caason Micropolar fluid*

IX. Equations governing angular velocity (M_{cm}), linear fluid velocity (u_{cm}), and temperature (T_{cm}) under above mentioned assumed constraints for present magnetohydrodynamic fluid flow are [18]:

Region of flow $(0 \le y \le k)$

$$\frac{\partial u_{cm}}{\partial t} = \frac{\kappa_{cm}}{\rho_{cm}}\frac{\partial M_{cm}}{\partial y} + \left[\frac{\mu_{cm}}{\rho_{cm}}\left(1+\frac{1}{\beta}\right) + \frac{\kappa_{cm}}{\rho_{cm}}\right]\frac{\partial^2 u_{cm}}{\partial y^2} - \frac{\sigma B_0^2(1+Bi\,Be)u_{cm}}{[(1+Bi\,Be)^2+B_e^2]\rho_{cm}} \quad (2)$$

$$\rho_{cm} j_{cm}\frac{\partial M_{cm}}{\partial t} = \gamma_{cm}\frac{\partial^2 M_{cm}}{\partial y^2} - \kappa_{cm}\left(2M_{cm} + \frac{\partial u_{cm}}{\partial y}\right) \quad (3)$$

$$\rho_{cm} C_{pcm}\frac{\partial T_{cm}}{\partial t} = K_{cm}\frac{\partial^2 T_{cm}}{\partial y^2} + \mu_{cm}\left(1+\frac{1}{\beta}\right)\left(\frac{\partial u_{cm}}{\partial y}\right)^2 + \kappa_{cm}\left(2M_{cm} + \frac{\partial u_{cm}}{\partial y}\right)^2 + \beta_{cm}\left(\frac{\partial M_{cm}}{\partial y}\right)^2 + \frac{\sigma B_0^2(1+Bi\,Be)(u_{cm})^2}{[(1+Bi\,Be)^2+Be^2]} \quad (4)$$

The investigation involves the examination of the conventional no-slip and hyper-stick situations that dissipate at the boundary, where the microrotation and velocity are designated. Initially both the channel walls are held at constant temperature. Upper and lower plate's temperatures are taken as T_{up} and T_{lp}, respectively. The prescribed initial and boundary conditions are represented as:

Initial conditions: defined at

$$t \le 0 \qquad u_{cm}(x,t) = M_{cm}(y,t) = 0 \quad T_{cm}(y,t) = 0,\ for\ 0 \le y \le k \quad (5)$$

Boundary conditions: defined at

$$\left.\begin{array}{ll} t > 0, \quad u_{cm}(0,t) = 0, & M_{cm}(0,t) = 0, \\ T_{cm}(0,t) = T_{lp}, & u_{cm}(k,t) = U_0, \\ M_{cm}(k,t) = -\frac{1}{2}\frac{\partial u_{cm}}{\partial y}, & T_{cm}(k,t) = T_{up} \end{array}\right\} \quad (6)$$

At

The non-dimensional parameters used are:

$$\left.\begin{array}{l} \bar{y} = \frac{y}{k}, \bar{x} = \frac{x}{k}, \bar{u}_{cm} = \frac{u_{cm}}{U_0}, \\ \bar{t} = \frac{tU_0}{k}, \bar{T}_{cm} = \frac{\bar{T}_{cm}-T_{lp}}{T_{up}-T_{lp}}, \\ \bar{M}_{cm} = \frac{M_{cm}k}{U_0}, \end{array}\right\} \quad (7)$$

We assume $\gamma_{cm} = (\mu_{cm} + \kappa_{cm}/2)j_{cm}$ with $j_{cm} = k^2$. When the bars are removed, the Eqs. (2)– (4) take on the following form

Region of flow (For Casson Micropolar fluid;$0 \le y \le 1$)

$$\frac{\partial u_{cm}}{\partial t} = \frac{\eta_{cm}}{Re}\frac{\partial M_{cm}}{\partial y} + \frac{1}{Re}\left(1 + \frac{1}{\beta} + \eta_{cm}\right)\frac{\partial^2 u_{cm}}{\partial y^2} - \frac{Ha^2(1+Bi.Be)u_{cm}}{Re[(1+Bi.Be)^2+Be^2]} \quad (8)$$

$$\frac{\partial M_{cm}}{\partial t} = \frac{1}{Re}\left[\left(1 + \frac{\eta_{cm}}{2}\right)\frac{\partial^2 M_{cm}}{\partial y^2} - \eta_{cm}\left(2M_{cm} + \frac{\partial u_{cm}}{\partial y}\right)\right] \quad (9)$$

$$\frac{\partial T_{cm}}{\partial t} = \frac{Ec}{Re}\left[\frac{1}{Pr.Ec}\frac{\partial^2 T_{cm}}{\partial y^2} + \left(1 + \frac{1}{\beta}\right)\left(\frac{\partial u_{cm}}{\partial y}\right)^2 + \eta_{cm}\left(2M_{cm} + \frac{\partial u_{cm}}{\partial y}\right)^2 + \delta_{cm}\left(\frac{\partial M_{cm}}{\partial y}\right)^2 + \frac{Ha^2(1+Bi\,Be)u_{cm}{}^2}{[(1+Bi\,Be)^2+Be^2]}\right] \quad (10)$$

Equations (5)-(6) describe initial and boundary conditions for $T_0 = 0,\quad T_{lp} = 0,\quad T_{up} = 1,\quad U_0 = 1\ and\ k = 1.$ In equation (8) to (10) the various parameters (refer nomenclature) are defined as: $Re = (\rho_{cm}U_0k^2)/\mu_{cm},\quad \eta_{cm} = (\kappa_{cm}/\mu_{cm}),\quad Ha^2 = (\sigma B_0^2k^2)/\mu_{cm},\quad Ec = \left(U_0/C_{pcm}\right), Cm = 1 + \frac{1}{\beta}\quad , Pr = (\mu_{cm}C_{Pcm})/K_{cm}, \delta_{cm} = (\beta_{cm}/\mu_{cm}k^2)$ is the applied time-dependent pressure gradient with time t > 0 acting in the direction of x-axis.

3 NUMERICAL SOLUTION

The region of flow for the Casson micropolar fluid in the horizontal channel is the interval [0,1]. The distribution of fluid velocities and temperature in this region is computed by partitioning the domains along the y-axis with step sizes of h and in time with step sizes of k.

$$0 = y_1 < y_2 < \ \dots\dots\ < y_{n-1} < y_n = 1,$$

Such that, on real axis $h = y_{i+1} - y_i$ *(11)*

Here $S_{iyy}(y_i, t)$ represent the second-order derivative and $S_{iy}(y_i, t)$ represent the first-order derivative of u_{cm}, M_{cm}, T_{cm} with respect to y_i as calculated at the nodes x_i at any given time.
considering $i = 1, 2, \dots\dots., n.\ S_{iy}(y_i, t) = \sum_{j=1}^{N} a^*{}_{ij} S_i\left(y_j, t\right) ; j = 1, 2, 3 \dots\dots.. N$

$$S_{iyy}(y_i, t) = \sum_{j=1}^{N} b^*{}_{ij} S_i\left(y_j, t\right) \text{ for } j = 1, 2, 3 \dots\dots.. N \quad (12)$$

The weight coefficients $b^*{}_{ij}$ and $a^*{}_{ij}$ represent the first and second-order derivatives, respectively, with respect to the y-coordinate.

These coefficients are calculated based on a cubic B-spline function, with specified knots as follows:

$$\vartheta_j = \frac{1}{h^3}\begin{cases} \left(y - y_{j-2}\right)^3, & y \in [y_{j-2}, y_{j-1}) \\ \left(y - y_{j-2}\right)^3 - 4\left(y - y_{j-1}\right)^3, & y \in [y_{j-1}, y_j) \\ \left(y_{j+2} - y\right)^3 - 4\left(y_{j+1} - y\right)^3, & y \in [y_j, y_{j+1}) \\ \left(y_{j-2} - y\right)^3, & y \in [y_{j+1}, y_{j+2}) \\ 0 & Otherwise \end{cases} \quad (13)$$

Basis in $[0, 1]$ are formed by $\vartheta_j\ with\ j = 1, 2, 3, \dots\dots, N + 1$. Calculation are done for

$$\psi_1 = \vartheta_1(y) - \vartheta_0(y) \quad (14)$$

$$\psi_2 = \vartheta_2(y) - \vartheta_0(y) \quad (15)$$

$$\psi_j = \vartheta_j(y), \quad \text{for } j = 3, 4, \dots\dots\dots, N - 2 \quad (16)$$

$$\psi_{N-1} = \vartheta_{N-1}(y) - \vartheta_{N+1}(y) \quad (17)$$

$$\psi_N = \vartheta_{N-1}(y) + \vartheta_{N+1}(y) \tag{18}$$

each node's using cubic B-spline functions as follows:

Here basis for said domain $[0, 1]$ are formed by set $\{\psi_1, \psi_2, \ldots\ldots\psi_N\}$. Coefficients $a^*{}_{ij}$, $b^*{}_{ij}$

are computed using function referred as updated cubic B-spline. The estimation of first order derivative is generated as:

$$\psi'_k(y_i) = \sum_{j=1}^{N} a^*{}_{ij}\, \vartheta_k(y_j) \begin{matrix} for\ i = 1, 2, \ldots\ldots N \\ k = 1, 2, \ldots\ldots\ldots N \end{matrix} \tag{19}$$

For first-knot point y_1:

$$\psi'_k(y_1) = \sum_{j=1}^{N} a^*{}_{1j}\, \vartheta_k(y_j) \begin{matrix} for\ i = 1, 2, \ldots\ldots N \\ k = 1, 2, \ldots\ldots\ldots N \end{matrix} \tag{20}$$

The system of equations generated is given as:

$$\begin{bmatrix} 6 & 1 & 0 & 0 & & & & & \\ 0 & 4 & 1 & 0 & \cdots & 0 & & 0 & \\ 0 & 1 & 4 & 1 & & & & & \\ & \vdots & & 0 & \ddots & 0 & & \vdots & \\ & & & & & 1 & 4 & 1 & 0 \\ & 0 & & 0 & \cdots & 0 & 1 & 4 & 0 \\ & & & & & 0 & 0 & 1 & 6 \end{bmatrix} \times \begin{bmatrix} a^*{}_{11} \\ a^*{}_{12} \\ a^*{}_{13} \\ \vdots \\ \vdots \\ a^*{}_{1N-2} \\ a^*{}_{1N-1} \\ a^*{}_{1N} \end{bmatrix} = \begin{bmatrix} -6/h \\ 6/h \\ 0 \\ \vdots \\ \vdots \\ 0 \\ 0 \\ 0 \end{bmatrix} \tag{21}$$

Similarly, the next node y_2:

$$\psi'_k(y_2) = \sum_{j=1}^{N} a^*{}_{2j}\, \vartheta_k(y_j) \begin{matrix} for\ i = 1, 2, \ldots\ldots N \\ k = 1, 2, \ldots\ldots\ldots N \end{matrix} \tag{22}$$

$$\begin{bmatrix} 6 & 1 & 0 & 0 & & & & & \\ 0 & 4 & 1 & 0 & \cdots & 0 & & 0 & \\ 0 & 1 & 4 & 1 & & & & & \\ & \vdots & & 0 & \ddots & 0 & & \vdots & \\ & & & & & 1 & 4 & 1 & 0 \\ & 0 & & 0 & \cdots & 0 & 1 & 4 & 0 \\ & & & & & 0 & 0 & 1 & 6 \end{bmatrix} \times \begin{bmatrix} a^*{}_{21} \\ a^*{}_{22} \\ a^*{}_{23} \\ \vdots \\ \vdots \\ a^*{}_{2N-2} \\ a^*{}_{2N-1} \\ a^*{}_{2N} \end{bmatrix} = \begin{bmatrix} -3/h \\ 0 \\ 3/h \\ 0 \\ \vdots \\ 0 \\ 0 \\ 0 \end{bmatrix} \tag{23}$$

After each $y_i's$, the system of last node y_N is expressed as

$$\begin{bmatrix} 6 & 1 & 0 & 0 & & & & & \\ 0 & 4 & 1 & 0 & \cdots & 0 & & 0 & \\ 0 & 1 & 4 & 1 & & & & & \\ & \vdots & & 0 & \ddots & 0 & & \vdots & \\ & & & & & 1 & 4 & 1 & 0 \\ & 0 & & 0 & \cdots & 0 & 1 & 4 & 0 \\ & & & & & 0 & 0 & 1 & 6 \end{bmatrix} \times \begin{bmatrix} a^*_{N1} \\ a^*_{N2} \\ a^*_{N3} \\ \cdot \\ \vdots \\ a^*_{NN-2} \\ a^*_{NN-1} \\ a^*_{NN} \end{bmatrix} = \begin{bmatrix} 0 \\ 0 \\ 0 \\ \cdot \\ \vdots \\ 0 \\ -6/h \\ 6/h \end{bmatrix} \quad (24)$$

The coefficients provided by the above systems' solution are $a^*_{11},\ a^*_{12}, \ldots.,\ a^*_{1N},\ a^*_{21},\ a^*_{22}, \ldots\ldots a^*_{2N},\ a^*_{N1},\ a^*_{N2}, \ldots\ldots,\ a^*_{NN}$. Then
value of weighted coefficients b^*_{ij} for $j = 1, 2, \ldots\ldots\ldots N$, $i = 1, 2, \ldots\ldots N$ are determined as:

$$b^*_{ij} = \begin{cases} 2a^*_{ij}\left(a^*_{ij} - \frac{1}{y_i - y_j}\right) & for\ i \neq j \\ -\sum_{i=1, i\neq j}^{N} b^*_{ij} & for\ i = j \end{cases} \quad (25)$$

The Runge-Kutta (SSP-RK43)[25] time-stepping system, which is reliable and effective at maintaining stability, was employed to solve. The differential equations system is then expressed in a simplified form as follows:

$$s_t = S(u_{cm}, M_{cm}, T_{cm}) \quad (26)$$

$$S_1 = S_0 + \frac{\Delta t}{2} \times S\left(u_{cm_0}, M_{cm_0}, T_{cm_0}\right) \quad (27)$$

$$S_2 = S_1 + \frac{\Delta t}{2} \times S\left(u_{cm_1}, M_{cm_1}, T_{cm_1}\right) \quad (28)$$

$$S_3 = (2/3)R_0 + \frac{S_1}{3} + \frac{\Delta t}{6} \times S\left(u_{cm_2}, M_{cm_2}, T_{cm_2}\right) \quad (29)$$

$$S_M = S_3 + \frac{\Delta t}{2} \times S\left(u_{cm_3}, M_{cm_3}, T_{cm_3}\right) \quad (30)$$

4 RESULTS AND DISCUSSION

Figure 2, Figure 8 illustrate graphical representations of the velocity and microrotation with time for micropolar Casson fluid moving via a horizontal duct. Over time, there is an observable increase in both the velocity and microrotation. Specifically, the velocity experiences a peak rise near the midpoint of the channel, while the microrotation shows a peak rise near the channel's top wall.

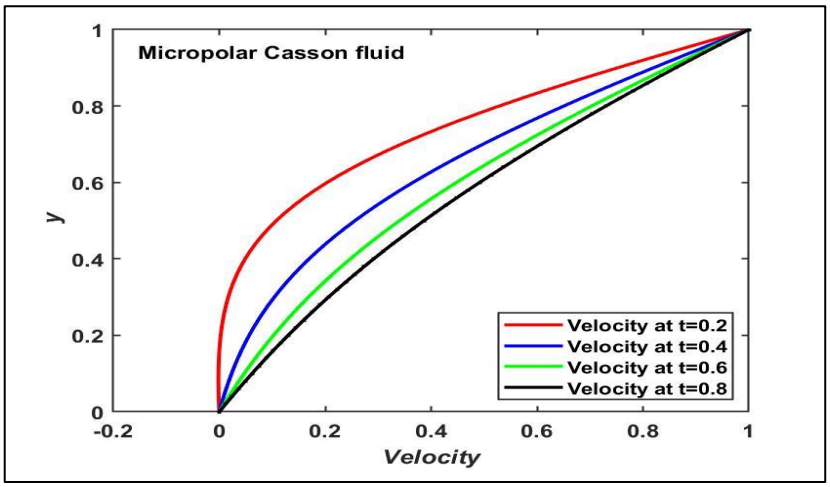

Figure 2 : *Linear velocity profile of fluid involving Couette flow with time variation and Ha^2=2; Cm=0.5; η_{cm}=0.5; Re=5; Be=2; Bi=2; Pr=2; Ec=0.5; δ_{cm}=2.*

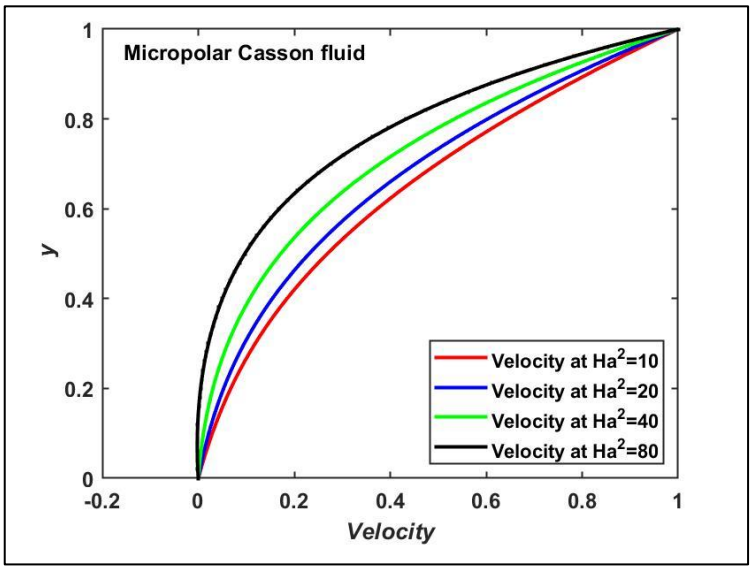

Figure 3 : *Linear velocity profile of fluid involving Couette flow with variation in square of Hartmann number (Ha^2) and t=0.5; Cm=0.5; η_{cm}=0.5; Re=5; Be=2; Bi=2; Pr=2; Ec=0.5; δ_{cm}=2.*

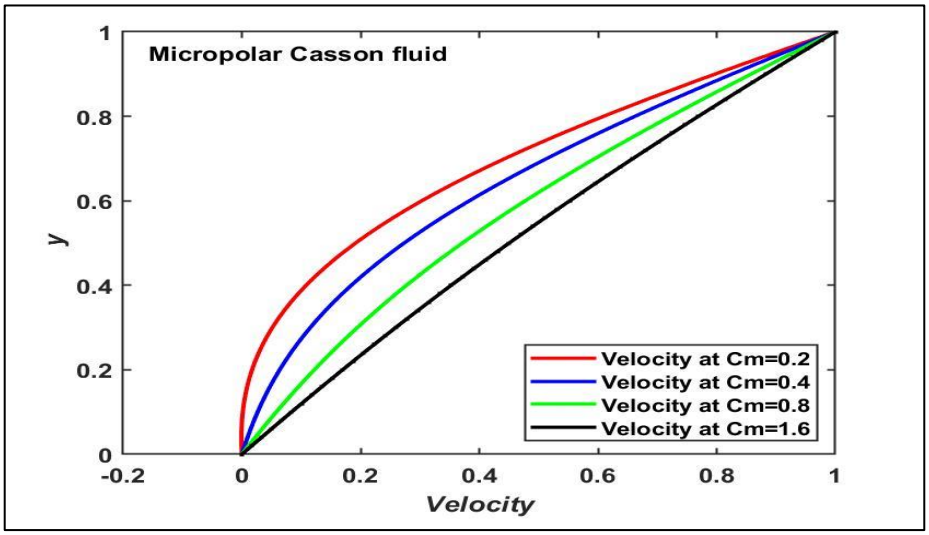

Figure 4: *Linear velocity profile of fluid involving Couette flow with variation in Casson micropolar parameter (Cm) and t=0.5; Ha^2=2; η_{cm}=0.5; Re=5; Be=2; Bi=2; Pr=2; Ec=0.5; δ_{cm}=2.*

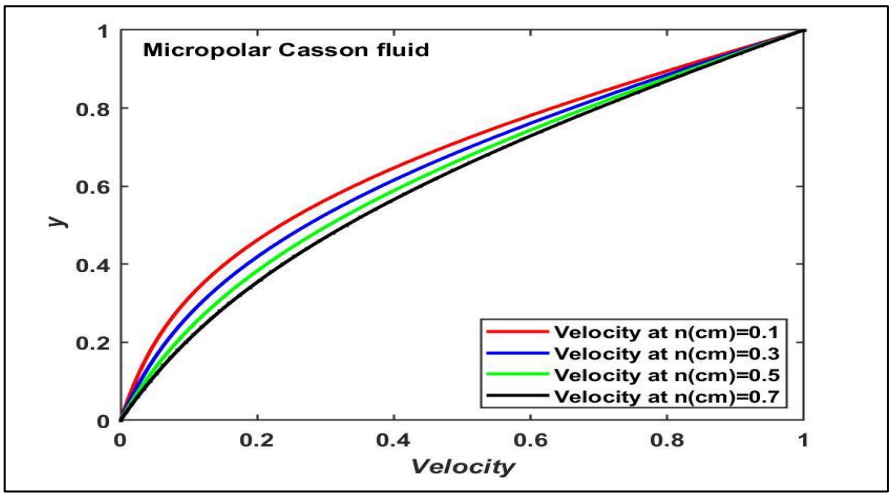

Figure 5: *Linear velocity profile of fluid involving Couette flow with variation in micropolar parameter (η_{cm}) and t=0.5; Ha^2=2; Cm=0.5; Re=5; Be=2; Bi=2; Pr=2; Ec=0.5; δ_{cm}=2.*

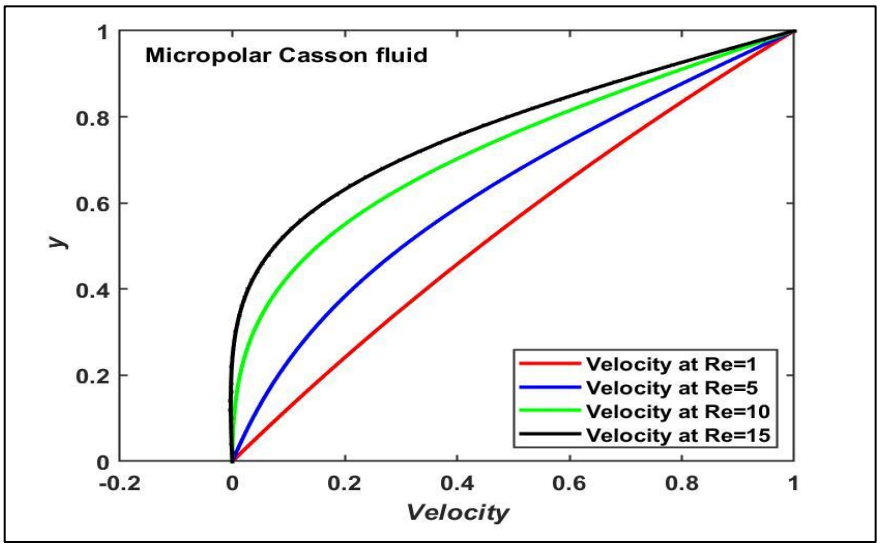

Figure 6: *Linear velocity profile of fluid involving Couette flow with variation in Reynold number (Re) and t=0.5; Ha^2=2; Cm=0.5; η_{cm}=0.5; Be=2; Bi=2; Pr=2; Ec=0.5; δ_{cm}=2.*

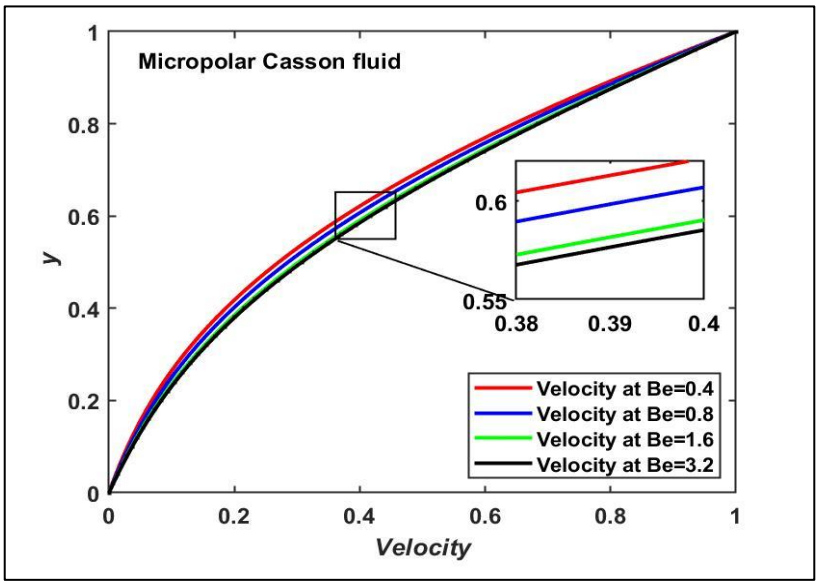

Figure 7: *Linear velocity profile of fluid involving Couette flow with variation in Hall parameter (Be) and t=0.5; Ha^2=2; Cm=0.5; Re=5; η_{cm}=0.5; Bi=2; Pr=2; Ec=0.5; δ_{cm}=2.*

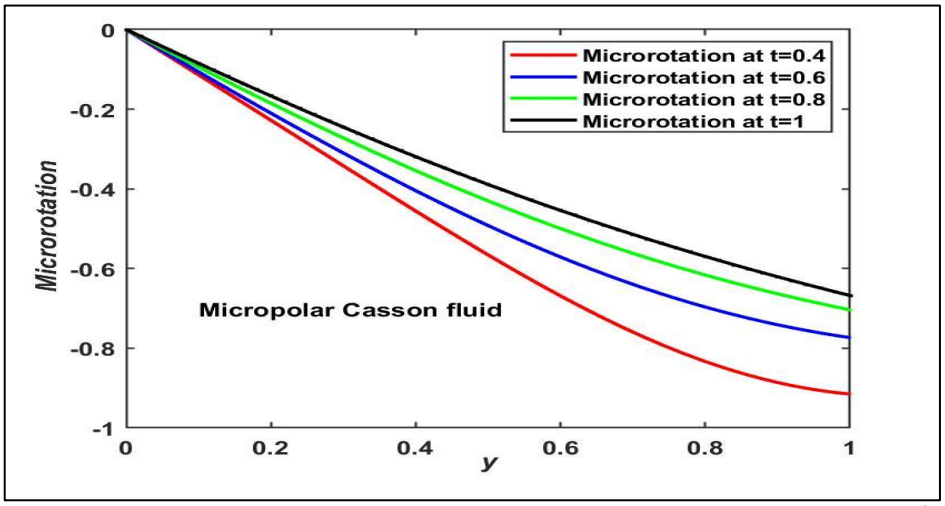

Figure 8: *Microrotation profile of fluid involving Couette flow with time variation and Ha^2=2; Cm=0.5; η_{cm}=0.5; Re=5; Be=2; Bi=2; Pr=2; Ec=0.5; δ_{cm}=2.*

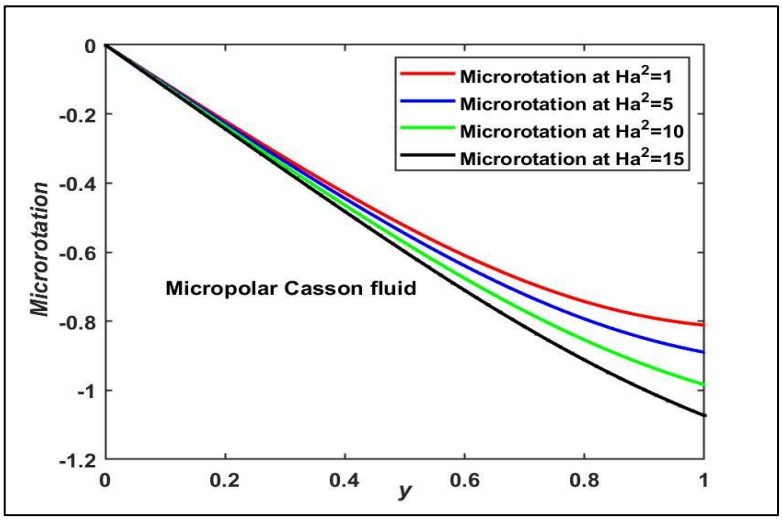

Figure 9: *Microrotation profile of fluid involving Couette flow with variation in square of Hartmann number (Ha^2) with t=0.5; Cm=0.5; η_{cm}=0.5; Re=5; Be=2; Bi=2; Pr=2; Ec=0.5; δ_{cm}=2.*

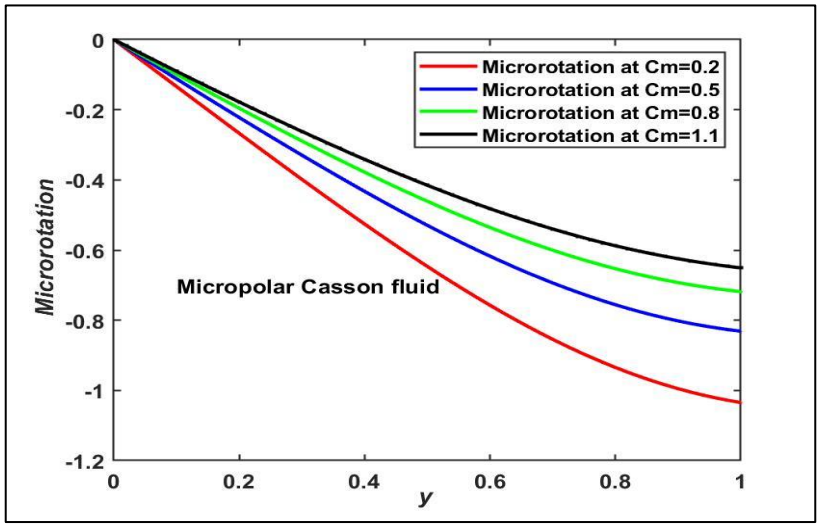

Figure 10: *Microrotation profile of fluid involving Couette flow with variation in Casson micropolar parameter (Cm) with t=0.5; Ha^2=2; η_{cm}=0.5; Re=5; Be=2; Bi=2; Pr=2; Ec=0.5; δ_{cm}=2.*

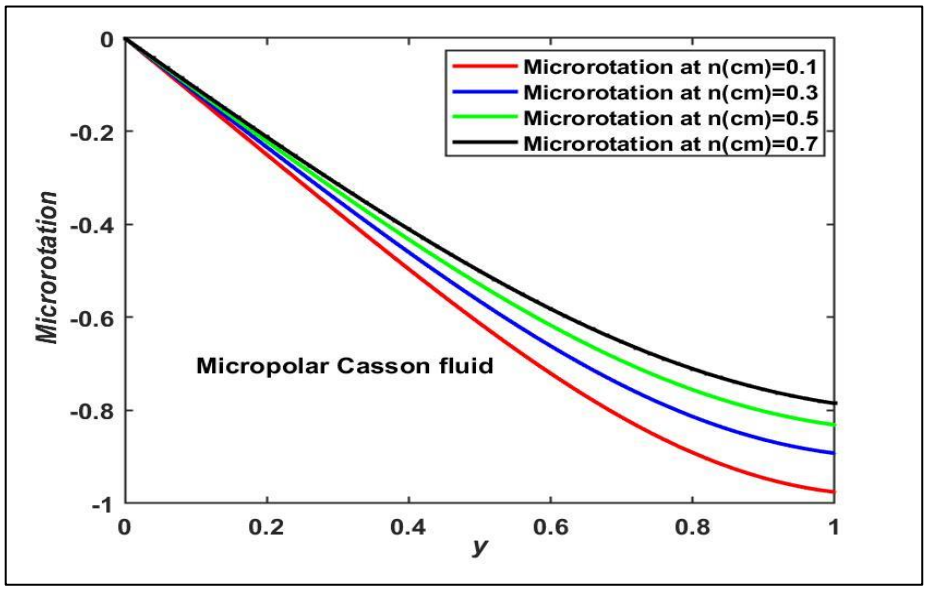

Figure 11: *Microrotation profile of fluid involving Couette flow with variation in micropolar parameter (η_{cm}) with t=0.5; Ha^2=2; Cm=0.5; Re=5; Be=2; Bi=2; Pr=2; Ec=0.5; δ_{cm}=2.*

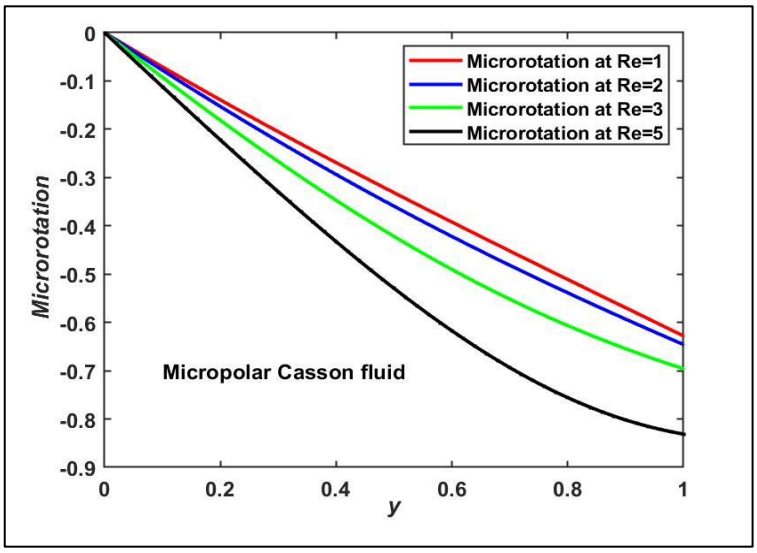

Figure 12: *Microrotation profile of fluid involving Couette flow with variation in Reynold number (Re) with t=0.5; Ha^2=2; Cm=0.5; η_{cm}=0.5; Be=2; Bi=2; Pr=2; Ec=0.5; δ_{cm}=2.*

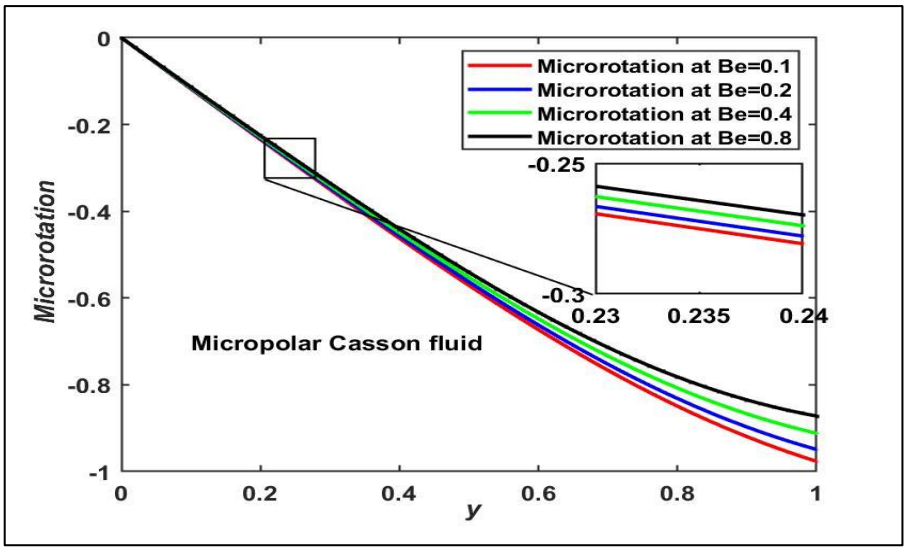

Figure 13: *Microrotation profile of fluid involving Couette flow with variation in Hall parameter (Be) with t=0.5; Ha^2=2; Cm=0.5; η_{cm}=0.5; Re=5; Bi=2; Pr=2; Ec=0.5; δ_{cm}=2.*

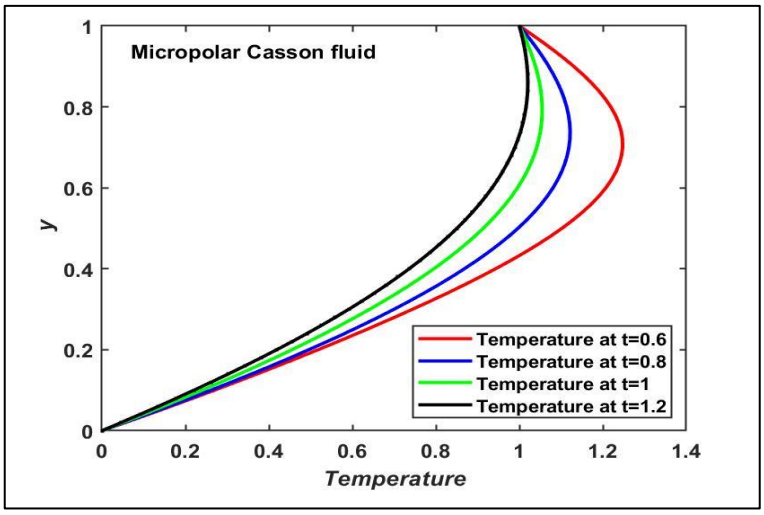

Figure 14: *Temperature profile of fluid involving Couette flow with time variation and Ha^2=2; Cm=0.5; η_{cm}=0.5; Re=5; Be=2; Bi=2; Pr=2; Ec=0.5; δ_{cm}=2.*

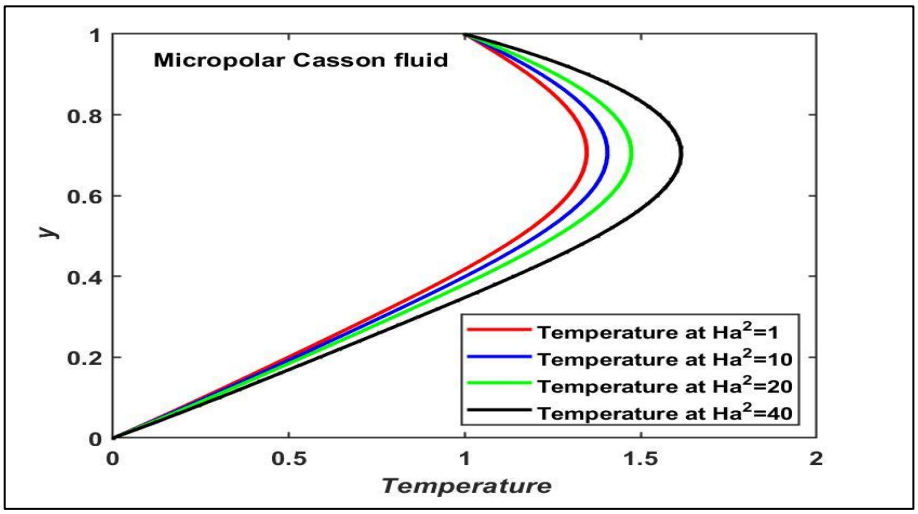

Figure 15: *Temperature profile of fluid involving Couette flow with variation in square of Hartmann number (Ha^2) with t=0.5; Cm=0.5; η_{cm}=0.5; Re=5; Be=2; Bi=2; Pr=2; Ec=0.5; δ_{cm}=2.*

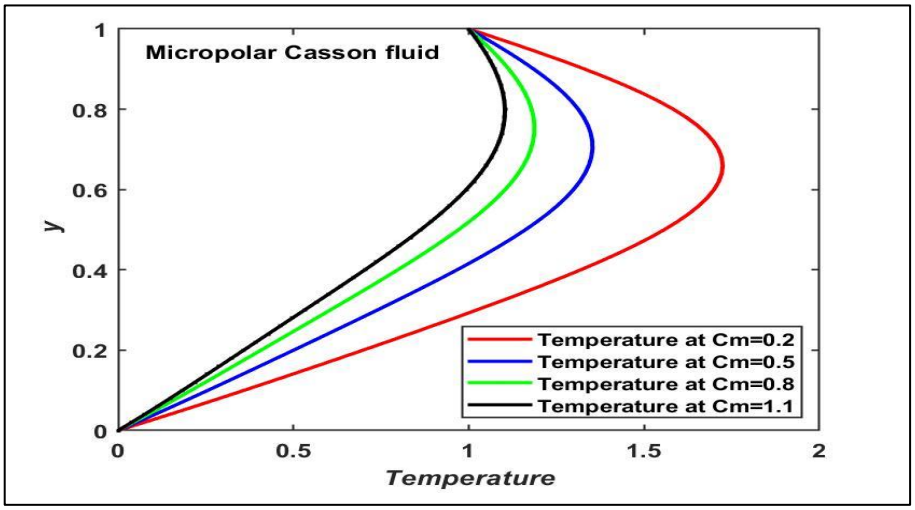

Figure 16: *Temperature profile of fluid involving Couette flow with variation in Casson micropolar parameter (Cm) with t=0.5; Ha^2=2; η_{cm}=0.5; Re=5; Be=2; Bi=2; Pr=2; Ec=0.5; δ_{cm}=2.*

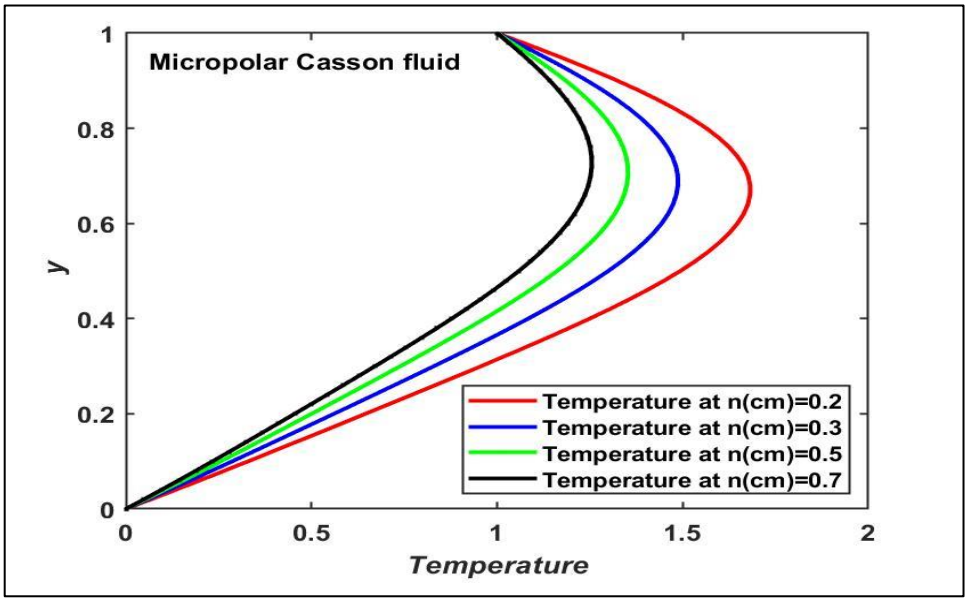

Figure 17: *Temperature profile of fluid involving Couette flow with variation in micropolar parameter (η_{cm}) with t=0.5; Ha^2=2; Cm=0.5; Re=5; Be=2; Bi=2; Pr=2; Ec=0.5; δ_{cm}=2.*

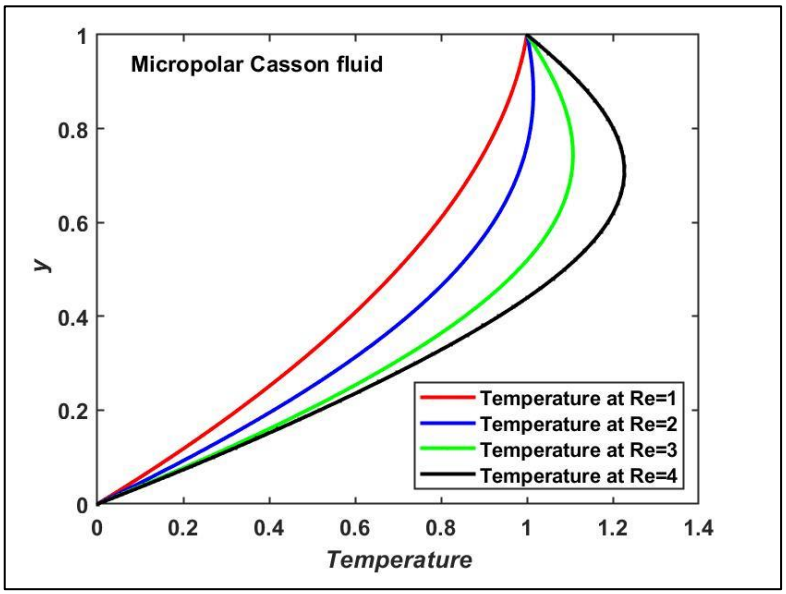

Figure 18: *Temperature profile of fluid involving Couette flow with variation in Reynold number (Re) with t=0.5; Ha^2=2; Cm=0.5; η_{cm}=0.5; Be=2; Bi=2; Pr=2; Ec=0.5; δ_{cm}=2.*

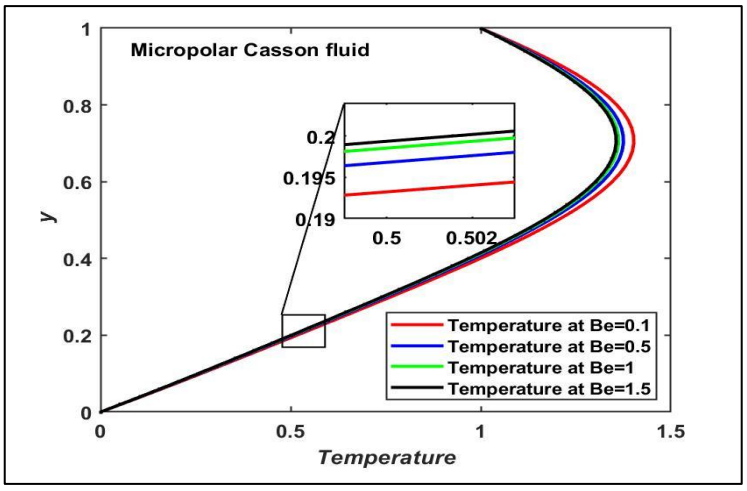

Figure 19: *Temperature profile of fluid involving Couette flow with variation in Hall parameter (Be) with t=0.5; Ha^2=2; Cm=0.5; η_{cm}=0.5; Re=5; Bi=2; Pr=2; Ec=0.5; δ_{cm}=2.*

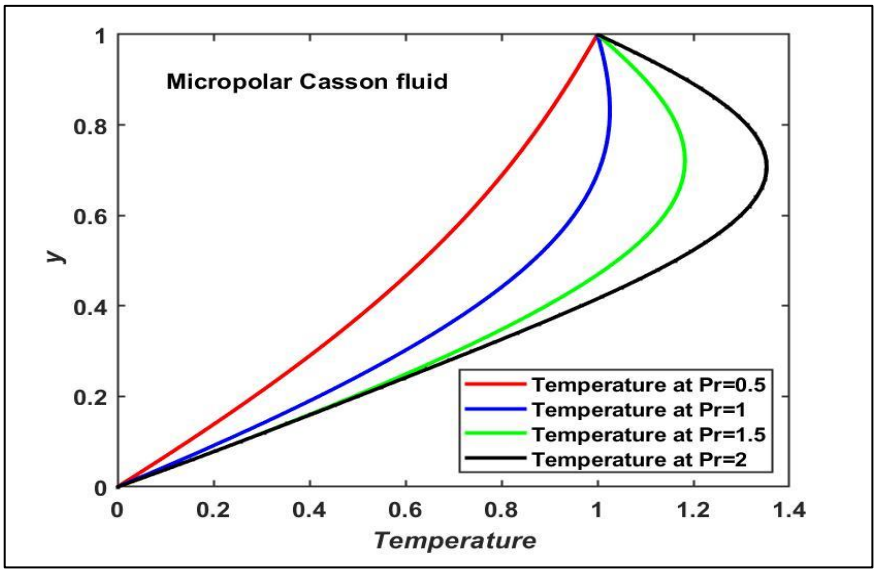

Figure 20: *Temperature profile of fluid involving Couette flow with variation in Prandtl number (Pr) with t=0.5; Ha2=2; Cm=0.5; η_{cm}=0.5; Re=5; Bi=2; Be=2; Ec=0.5; δ_{cm}=2.*

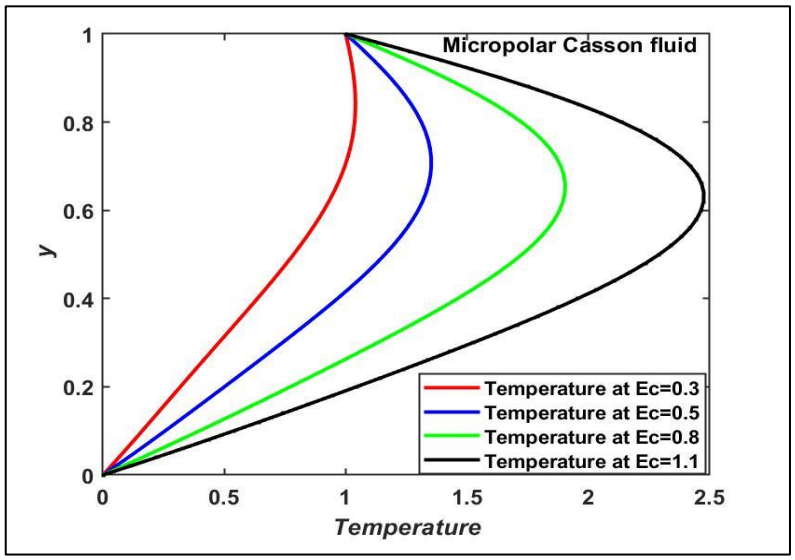

Figure 21: *Temperature profile of fluid involving Couette flow with variation in Eckert number (Ec) with t=0.5; Ha2=2; Cm=0.5; η_{cm}=0.5; Re=5; Bi=2; Be=2; Pr=2; δ_{cm}=2.*

The present study involves flow of micropolar Casson fluid via a horizontal channel, an inverse relationship between the Ha^2 and the linear velocity and microrotation is apparent, as demonstrated in Figure 3 and Figure 9. The Hartmann number, a dimensionless parameter representing the ratio two forces representing magnetic force to viscous force respectively within the fluid, increases the dominance of viscous forces as it rises, leading to a decrease in angular and linear velocities.

The Casson micropolar parameter is represented by $Cm = (1 + 1/\beta)$. Increase in the value parameter reduces the yield stress, which in turn allows the fluid to flow more easily. Consequently, the enhanced flow results an increment in both the microrotation and velocity of the Casson micropolar fluid as illustrated in Figure 4 and Figure 10.

A rise in the micropolar parameter $\eta_{cm} = \frac{\kappa_{cm}}{\mu_{cm}}$ is known to reduce the resistance to flow within the fluid, as it promotes the rotation and deformation of the microstructures within the fluid. This reduction in resistance leads to an increase in the velocity profile as observed in Figure 5. Also, as observed in Figure 11 increase in microrotation is due to the reason that an increment in the micropolar parameter causes the alignment of the fluid's microstructures in a matching manner to fluid's angular momentum vector. Thus, increasing the fluid's microrotation profile.

The decrease in the velocity and microrotation profile of a Casson micropolar fluid with an increase in Reynolds number as depicted in Figure 6 and Figure 12 can be explained by the dominant role of inertial forces. With rise in Reynolds number $\left(Re = \frac{\rho_1 U_0 h^2}{\mu_1}\right)$, the viscous forces become less significant than the inertial forces, leading to a reduction in the fluid's mean velocity due to increased fluctuations in the flow. Additionally, the alignment of the microstructures within the fluid decreases with increasing Reynolds number, resulting in a decrease in the fluid's microrotation profile due to reduced microstructure alignment.

As observed in Figure 7, Figure 13, the Hall parameter (Be) in a Casson micropolar fluid influences the flow behavior through its interaction with the fluid's microstructure. A rise in (Be) decreases the internal friction of fluid, resulting in an increment in the velocity. Furthermore, the magnetic field induced by the Hall effect causes an alignment of the microstructures to the fluid's angular momentum vector, increasing the fluid's microrotation profile.

The decrease in temperature profile with time as observed in Figure 14, is attributed to the convective heat transfer mechanism combined with the decreased heat transfer rate as a result of high viscosity of the Casson micropolar fluid.

The increase in temperature profile with square of Hartmann number as observed in Figure 15, can be attributed to a combination of Joule heating due to induced electric current and reduced heat transfer rate due to the high viscosity of Casson micropolar fluid.

The Casson Micropolar parameter and temperature profile of a Casson micropolar fluid has an inverse relation as depicted in Figure 16. An increase in $Cm = (1 + (1/\beta))$ increases the fluid's viscosity, thereby reducing

the rate of heat transfer from the fluid to the channel walls. This reduction in heat transfer rate results in a decrement in the fluid's temperature profile.

The decrease in temperature profile due to an increase in the micropolar parameter (η_{cm}) for a Casson micropolar fluid may be due to the change in flow behavior, viscosity, and thermal conductivity induced by the degree of microstructure and small-scale rotation within the fluid as depicted in Figure 17.

Rise in temperature with an increment in the Reynolds number is observed in Figure 18. With the increases in Reynolds number, the lower values of viscous forces over inertial forces lead to a transition from laminar to turbulent flow. Turbulent flow is typically associated with higher heat transfer rates due to enhanced fluid mixing. Therefore, the increase in temperature profiles is observed with an increase in Reynolds number.

Temperature reduction of micropolar Casson fluid with rise in Hall parameter value may be due to the reason that when the Hall parameter increases, magnetic field becomes stronger, resulting an increase in the Lorentz force. This force acts on the fluid, causing it to move in a circular motion perpendicular to the direction of flow. This circular motion reduces the flow velocity and, therefore, variation in temperature of fluid results as shown in Figure 19.

The fluid's thermal diffusivity increases as the Prandtl number rises, by which the rate of heat transmission gets accelerated. The fluid's temperature profile may rise as a result of this rise in the heat transfer rate as observed in Figure 20.

Figure 21 the relationship between temperature development within a horizontal channel with respect to Eckert number (Ec) is depicted. The Ec is a measure of the kinetic energy dissipated due to internal friction. As the value of Ec increases, the conversion of mechanical energy to thermal energy increases as well, resulting in a direct correlation between the temperature gradient and Ec.

5 CONCLUSION

The study model investigates the dependency on magnetic field and viscous heating on the Couette flow of micropolar Casson fluids in a horizontal channel with regard to heat transfer and applied magnetic field. To study the dynamics of the flow inside the horizontal channel, system of partial differential equations is developed. The efficient differential quadrature method with modified cubic B-spline has been utilized to conduct a numerical analysis of the transformed dimensionless boundary value problem. The temperature profiles have all been thoroughly visualized, together with their linear and angular velocities. The principal findings of the analysis are outlined in the list of points as:

I. A rise in the micropolar Casson parameter, the micropolar parameter and Hall parameter leads to an increase in both the velocity and microrotation profiles of the fluid, while an increase in Square of Hartmann number and Reynolds number results in a decrease in these profiles.
II. Temperature profiles decrease with time due to convective heat transfer and high viscosity, but may increase with the square of the Hartmann number due to Joule heating and reduced heat transfer rate.
III. The temperature profile also reduces with a rise in the micropolar, Casson micropolar and Hall parameters, but may increase with the Prandtl number, Eckert and Reynold number.

The findings of the study provide a scientific basis for the creation and improvement of numerical models and simulations. In a variety of systems, including the design of microfluidic devices, electronic cooling systems and material processing methods, these models can be used to forecast fluid flow and heat transfer. These models can result in increased effectiveness and efficiency in many engineering applications.

REFERENCES

1. Z. Mehmood, R. Mehmood, and Z. Iqbal, "Numerical Investigation of Micropolar Casson Fluid over a Stretching Sheet with Internal Heating," *Commun. Theor. Phys.*, 2017, doi: 10.1088/0253-6102/67/4/443.
2. S. M. Upadhya, C. S. K. Raju, K. Vajravelu, and D. Guinovart-Sanjuán, "Analysis of Micro-Hybrid and Casson-Hybrid Nano-Convective and Radiative Fluid Flow in an Inclined Channel," *J. Nanofluids*, 2022, doi: 10.1166/jon.2023.1916.
3. N. Abbas and W. Shatanawi, "Heat and Mass Transfer of Micropolar-Casson Nanofluid over Vertical Variable Stretching Riga Sheet," *Energies*, 2022, doi: 10.3390/en15144945.
4. M. D. Shamshuddin and W. Ibrahim, "Finite element numerical technique for magneto-micropolar nanofluid flow filled with chemically reactive casson fluid between parallel plates subjected to rotatory system with electrical and Hall currents," *Int. J. Model. Simul.*, 2022, doi: 10.1080/02286203. 2021.2012634.
5. N. A. M. Noor, M. A. Admon, and S. Shafie, "Unsteady MHD Squeezing Flow of Casson Fluid Over

Horizontal Channel in Presence of Chemical Reaction," *J. Adv. Res. Fluid Mech. Therm. Sci.*, 2022, doi: 10.37934/ arfmts. 92.2.4960.
6. Z. Iqbal and M. Saleem, "Convective heat transport features of Darcy Casson fluid flow in a vertical channel: a Lie group approach," *Waves in Random and Complex Media*, 2022, doi: 10.1080/17455030.2022.2142694.
7. B. V. Shilpa, D. V. Chandrashekhar, P. A. Dinesh, C. V. Vinay, C. G. Raghavendra, and B. J. Gireesha, "Soret and Dufour effect on convection flow of Casson fluid in a channel," *J. Therm. Anal. Calorim.*, 2022, doi: 10.1007/ s10973-022-11707-8.
8. F. Hussain, M. Nazeer, I. Ghafoor, A. Saleem, B. Waris, and I. Siddique, "PERTURBATION SOLUTION OF COUETTE FLOW OF CASSON NANOFLUID WITH COMPOSITE POROUS MEDIUM INSIDE A VERTICAL CHANNEL," *Nanosci. Technol.*, 2022, doi: 10.1615/ NanoSci TechnolIntJ. 2022038799.
9. B. J. Gireesha and L. Anitha, "Repercussion of Hall effect and nonlinear radiation on Couette-Poiseuille flow of Casson-Williamson fluid through upright microchannel," *Appl. Math. Mech. (English Ed.*, 2022, doi: 10.1007/ s10483-022-2929-8.
10. S. Gajbhiye, A. Warke, and R. Katta, "Role of electromagnetic analysis in radiative immiscible Newtonian and non-Newtonian fluids through a microchannel with chemical reactions," *Heat Transf.*, 2022, doi: 10.1002/ htj.22631.
11. P. Mondal, D. K. Maiti, G. C. Shit, and G. Ibáñez, "Heat transfer and entropy generation in a MHD Couette–Poiseuille flow through a microchannel with slip, suction–injection and radiation," *J. Therm. Anal. Calorim.*, 2022, doi: 10.1007/s10973-021-10731-4.
12. N. Abbas, W. Shatanawi, and K. Abodayeh, "Computational Analysis of MHD Nonlinear Radiation Casson Hybrid Nanofluid Flow at Vertical Stretching Sheet," *Symmetry (Basel).*, 2022, doi: 10.3390/sym14071494.
13. N. Abbas, S. Nadeem, and M. N. Khan, "Numerical analysis of unsteady magnetized micropolar fluid flow over a curved surface," *J. Therm. Anal. Calorim.*, 2022, doi: 10.1007/s10973-021-10913-0.
14. H. R. Kataria, H. R. Patel, and R. Singh, "Effect of magnetic field on unsteady natural convective flow of a micropolar fluid between two vertical walls," *Ain Shams Eng. J.*, vol. 8, no. 1, pp. 87–102, 2017, doi: 10.1016/ j.asej.2015.08.013.
15. B. Widodo, I. Anggriani, D. A. Khalimah, F. D. S. Zainal, and C. Imron, "Unsteady boundary layer magnetohydrodynamics in micropolar fluid past a sphere," *Far East J. Math. Sci.*, 2016, doi: 10.17654/MS1000 20291.
16. R. Kodi and O. Mopuri, "Unsteady MHD oscillatory Casson fluid flow past an inclined vertical porous plate in the presence of chemical reaction with heat absorption and Soret effects," *Heat Transf.*, 2022, doi: 10.1002/htj.22327.
17. H. R. Patel, "Soret and heat generation effects on unsteady MHD Casson fluid flow in porous medium," *Waves in Random and Complex Media*, 2022, doi: 10.1080/17455030. 2022. 2030500.
18. H. T. Alkasasbeh, "Numerical solution of micropolar casson fluid behaviour on steady MHD natural convective flow about a solid sphere," *J. Adv. Res. Fluid Mech. Therm. Sci.*, 2018.
19. L. Panigrahi, J. Panda, K. Swain, and G. C. Dash, "Heat and mass transfer of MHD Casson nanofluid flow through a porous medium past a stretching sheet with Newtonian heating and chemical reaction," *Karbala Int. J. Mod. Sci.*, 2020, doi: 10.33640/ 2405-609X.1740.
20. T. Sharma, P. Sharma, and N. Kumar, "Chemical reactive magnetized fluid flow through a vertical channel due to heat source and thermal radiation effects," *Mater. Today Proc.*, 2022, doi: 10.1016/j.matpr. 2022. 10. 298.
21. T. Sharma, P. Sharma, and N. Kumar, "Study of dissipative MHD oscillatory unsteady free convective flow in a vertical channel occupied with the porous material in the presence of heat source effect and thermal radiation," 2022, doi: 10.1088/1742-6596/2178/1/ 0120 12.
22. T. Sharma, P. Sharma, and N. Kumar, "Entropy generation in thermal radiative oscillatory MHD couette flow in the influence of heat source," 2021, doi: 10.1088/1742-6596/ 1849/1/012023.
23. T. Sharma, P. Sharma, and N. Kumar, "Analysis of Entropy Generation Due to MHD Natural Convective Flow in an Inclined Channel in the Presence of Magnetic Field and Heat Source Effects," *Bionanoscience*, 2019, doi: 10.1007/s12668-019-00632-0.
24. R. C. Mittal and R. Rohila, "Numerical simulation of reaction-diffusion systems by modified cubic B-spline differential quadrature method," *Chaos, Solitons and Fractals*, 2016, doi: 10.1016/ j.chaos. 2016. 09.007.
25. G. Arora and B. K. Singh, "Numerical solution of Burgers' equation with modified cubic B-spline

differential quadrature method," *Appl. Math. Comput.*, 2013, doi: 10.1016/j.amc.2013.08.071.
26. H. A. Attia, W. Abbas, and M. A. M. Abdeen, "Ion slip effect on unsteady Couette flow of a dusty fluid in the presence of uniform suction and injection with heat transfer," *J. Brazilian Soc. Mech. Sci. Eng.*, vol. 38, no. 8, pp. 2381–2391, 2016, doi: 10.1007/s40430-015-0311-y.